



Control of a Spherical Robot Rolling Over Irregular Surfaces


Sergio-Daniel Sanchez-Solar

(Computer Science Department, Instituto Nacional de Astrofísica, Óptica y Electrónica (INAOE),
Luis Enrique Erro 1, 72840, Tonantzintla. Puebla, México
 <https://orcid.org/0000-0002-4722-367X>, ssanchez37@inaoep.mx)

Gustavo Rodriguez-Gomez

(Computer Science Department, Instituto Nacional de Astrofísica, Óptica y Electrónica (INAOE),
Luis Enrique Erro 1, 72840, Tonantzintla. Puebla, México
 <https://orcid.org/0000-0002-4925-8892>, grodrig@inaoep.mx)

Jose Martinez-Carranza

(Computer Science Department, Instituto Nacional de Astrofísica, Óptica y Electrónica (INAOE),
Luis Enrique Erro 1, 72840, Tonantzintla. Puebla, México
 <https://orcid.org/0000-0002-8914-1904>, carranza@inaoep.mx)

Abstract: Pendulum-Driven Spherical Robots are a type of spherical robot whose motion is achieved by controlling two motors for longitudinal and lateral motion. This configuration makes the robot a non-holonomic system, which impedes it from navigating directly towards a target. In addition, controlling its motion on inclined irregular surfaces is also an issue that has not received much attention. In this work, we addressed these two issues by proposing a methodology to control both motors using PID controllers. However, we propose tuning the controller's gains using stochastic signals for the longitudinal controller because by varying the motor's torque, the robot is more susceptible to destabilization in combination with a classical gain tuning methodology for the second controller. Our results indicate that this enables the robot to perform motion on inclined irregular surfaces. We also propose using semicircular trajectories to plan the robot's motion to reach a target successfully even when moving on inclined irregular surfaces. We have carried out experiments in the Webots simulator, showing that our approach does not overshoot while reaching a settling time of almost 0. These results outperform the Ziegler-Nichols PID controller.

Keywords: Spherical Robot, Irregular Surfaces, Variable Slope, Stochastic Signals, PID Control, Non-holonomic System

Categories: I.2.9, I.6, J.0, J.6

DOI: 10.3897/jucs.89703

1 Introduction

Mobile robots have been widely used for exploring unknown environments, both on the land and in space. They must deal with harsh conditions that compromise their integrity, such as dust, humidity, and water. Spherical robots are a type of mobile robot able to overcome those conditions. They are equipped with an external shell that protects their internal components even from collisions, and the robot is not overturned due to their spherical shape [Koshiyama and Yamafuji 93]. These features make them

appropriate for unmanned vehicle applications to be deployed on hostile or irregular surfaces. Furthermore, this type of robot can reduce friction and energy consumption for its motion since they have minimum contact with the support surface.

According to their motion mechanism, the taxonomy of the spherical robots considers a barycenter offset, shell transform, and conservation of angular moment [Chase and Pandya 12]. This work focuses on a Pendulum-Driven Spherical Robot (PDSR) with a barycenter offset, shifting the center mass through a pendulum that rotates around the shaft. A drawback of this robot is that movement is non-holonomic, which means its global degrees of freedom are greater than the degrees of freedom that can be controlled, which represents a significant challenge in the design of trajectories planning.

A PDSR has two motors to produce the robot's locomotion, one of them is placed at one end of the transversal shaft to produce longitudinal motion. At the same time, the other is located at the center of the transversal shaft to make steering motion. Each motor is controlled by a PID that regulates the torque supplied to them. The PID control was tuned using stochastic signals for the longitudinal motor, making it more robust to disturbances because it is needed to manipulate the torque. According to the tests performed, a slight change in such value is capable of destabilizing the system. In contrast, the steering motor's PID control was tuned classically due to the value being manipulated is the angular velocity, and opposite to the first motor, it does not affect the robot's behavior abruptly. PID controllers was consider to take advantage of their benefits, such as the less amount of sensors to be installed inside the spherical shell, resulting in less energy consumption and, therefore, greater autonomy to perform space exploration in hostile environments.

Although extensive research has been conducted in this area, there are still some shortcomings to be addressed. For instance, a PDSR has difficulties performing locomotion on inclined slopes [Chase and Pandya 12]. In addition, their non-holonomic constraints do not allow them to reach goals directly or perform the backward motion. Motivated by these constraints, in this work, we propose an approach to enable a PDSR to follow trajectories considering the turning radius associated with its movement when it is rolling over a surface whose slope is changing continuously. Thus, by proposing semicircular trajectories, the robot becomes capable of reaching goals on inclined surfaces with the caveat that more time may be required to execute the motion. Figure 1 depicts the stages this work covers. In phase one, the mathematical model is obtained which is used to tune the stochastic PID and classic PID controllers in second stage. The third stage focus on implement both controllers to enable PDSR to roll over irregular surfaces and track the proposed trajectories. Finally, in the last stage, simulation results using Webots as virtual environment are carried out.

This paper is organized as follows: In section 2, previous work done by other authors related to the scope of this work is presented. Section 3 describes the mathematical model of the spherical robot driven by one simple pendulum used to realize this project. The techniques to make the robot able to deal with inclined and irregular surfaces are exposed in Section 4. The proposed approach for tracking the trajectories to be followed by the system is exposed in Section 5. Section 6 presents the results obtained by implementing the system in a virtual environment, which in this case is Webots©. The conclusions reached from the analysis of the results are discussed in Section 7.

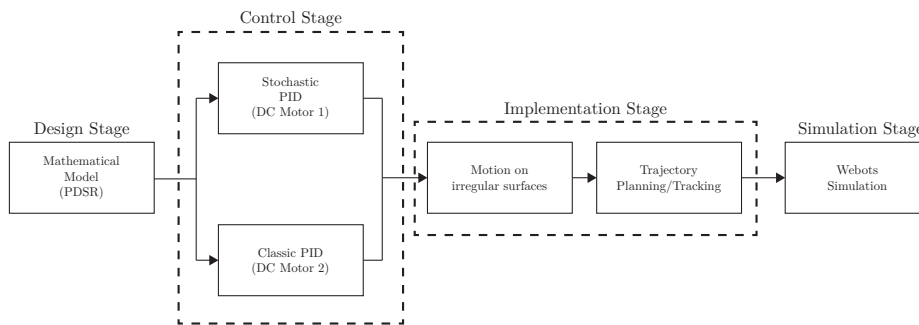


Figure 1: Proposed work flow diagram of PDSR rolling over irregular surfaces

2 Related work

Spherical robots moving on inclined planes have been studied by some authors, especially those whose slope does not change over time. A spherical robot model with an axisymmetric pendulum at the transversal shaft of the robot was proposed in [Ivanova et al. 18b]. The robot can roll over rough surfaces without slipping, and it can perform longitudinal motion and steering motion to perform some basic trajectories like a straight line and a circle. The algorithm to control the robot is a pure pursuit controller that considers a path as the reference and forces the system to follow it considering its current direction of motion and the desired direction [Ivanova et al. 18a]. The analysis of wobbling and precession of a spherical robot driven by one pendulum while it executes turning motion with a moderate forward speed was performed [Singhal et al. 23]. Also, the dynamic model of a spherical robot driven by a two-degree-of-freedom pendulum was derived using Boltzmann-Hamel equation and it was controlled using an adaptive sliding mode control to track two different trajectories [Tian et al. 23]. The stability of the controller was proved using Lyapunov Theorem.

Path following control of a spherical robot driven by one simple pendulum using Lyapunov stability theorem and exponential reaching law has been proposed in [Yu et al. 13]. The proposed trajectories are straight lines, circles, and a piecewise path. Geometric PID control and feedback regularization methods were applied to control the trajectory tracking of hoop robots rolling on an inclined plane [Madhushani et al. 17]. These robots consist of a circular frame containing a drive mechanism to enable the frame to roll over inclined surfaces and, even the authors mention the driving mechanism could be one simple pendulum, they focus their results in a circular frame containing a cart. Different locomotion mechanisms are used on robots, such as an internal vehicle and a simple pendulum. In [Aalipour et al. 20] a nonlinear control is developed to control the two-dimensional motion of a spherical robot driven by a pendulum, and the rotation angle and the ideal angle are compared. Heuristic fuzzy controller and PID control are used by Roozegar et al. [Roozegar and Mahjoob 17] to balance a spherical robot and perform longitudinal motion on an inclined plane. Genetic algorithms tune PID gains. An hybrid method for path planning for spherical robots based on pendulum called A^* has been improved to generate feasible and achievable paths than can be followed in line with low time cost [Zhang et al. 21]. They are capable of calculate the minimal area for rotation of a spherical robot. Yaw angle prediction has been considered to design a controller using Fuzzy-PID technique to enable a spherical robot to autonomously

change its parameters to roll on different environments [Wang et al. 21].

Rough terrains or variable slopes are considered in other works. For example, Roozegar et al. [Roozegar et al. 17] proposed to use a terminal sliding mode control on a spherical robot rolling on an inclined plane whose slope is variable. They consider that the angle of the slope is varying by $\frac{\pi}{8} + \frac{\pi}{12} \sin(\frac{\pi t}{40})$ and the robot performs longitudinal motion. Moazami et al. [Moazami et al. 19b, Moazami et al. 19a] consider that spherical robot rolls over rough surfaces, and a pure pursuit method is utilized to deal with the path tracking control problem of the model. A circular trajectory and a path with sharp vertices are used to be followed by the robot. A dynamic analysis of the behavior of a spherical robot that rolls over rough terrains and inclined planes is also carried out in [Yu et al. 11] where circular trajectories on both surfaces are conducted. Bio-inspired techniques for overcoming irregular surfaces have been proposed in previous works. Ocampo et al. [Ocampo-Jiménez et al. 14] proposed a sea urchin-like robot based on a spherical robot driven by a pendulum equipped with telescopic legs inside the robot that can be extended to help the robot to overcome hollows in the terrain and obstacles, as well as deal with rough terrains.

3 Mathematical model of the spherical robot

Some mathematical models that describe pendulum-driven spherical robot have been proposed by Laplante [Laplante et al. 07], Nagai [Nagai 08], Roozegar [Roozegar and Mahjoob 17, Roozegar et al. 17], Ocampo [Ocampo 10] and Halme [Halme et al. 96]. We selected the spherical robot model proposed by Roozegar and adapted it to our requirements. The robot model is obtained by the Euler–Lagrange method, which allows obtaining it through the system’s energies. In this case, it is essential to assume that the spherical robot is rolling over a rigid flat surface and does not slip. Figure 2 shows a schematic side view of a spherical robot. It depicts angles, velocities, masses, and moments. The parameters of the spherical robot are given in Table 1.

The dynamic model of the spherical robot is derived via the Lagrange approach. The Lagrangian function of the system is $\mathcal{L} = T - U$ where T and U are the kinetic and potential of the system, respectively. The kinetic energy T includes the kinetic and the rotational energy of the system, and it is given by (1), where K_s and R_s are the kinetic and rotational energies of the sphere and K_p and R_p are the kinetic and rotational energies of the pendulum, respectively. The potential energy is the sum of the potential energy of the sphere and the potential energy of the pendulum around its centroid of the sphere, as it is shown in (2).

$$T = K_s + K_p + R_s + R_p \quad (1)$$

$$U = U_s + U_p \quad (2)$$

The following equations give the kinetic energies:

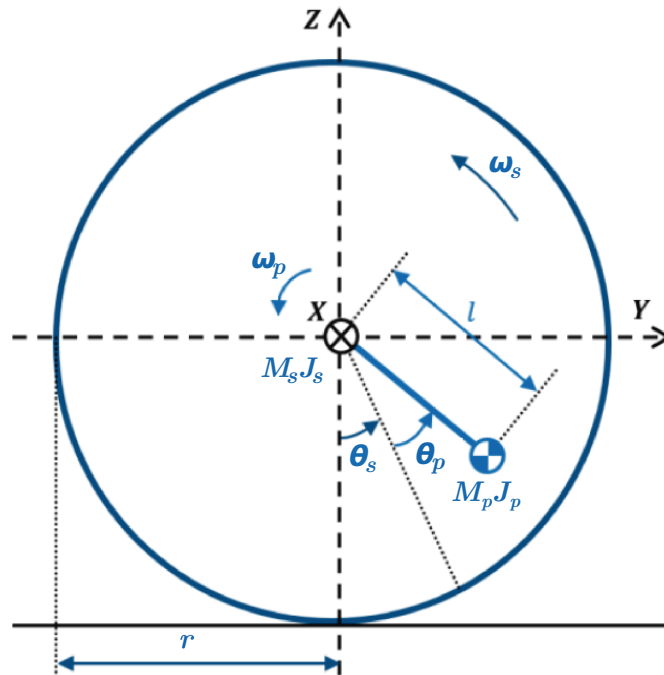


Figure 2: Spherical robot side view

$$K_s = \frac{1}{2} M_s (r \omega_s)^2$$

$$K_p = \frac{1}{2} M_p \left((r \omega_s - l (\omega_s + \omega_p) \cos(\theta_s + \theta_p))^2 + (l (\omega_s + \omega_p) \sin(\theta_s + \theta_p))^2 \right)$$

$$R_s = \frac{1}{2} J_s \omega_s^2, \quad R_p = \frac{1}{2} J_p (\omega_s + \omega_p)^2$$

The potential energy of the sphere U_s is 0 because it is on the surface it is rolling on. The potential energy of the pendulum changes since its height variations fitting to its angle, as shown in the following equations:

$$U_s = 0, \quad U_p = -M_p g l \cos(\theta_s + \theta_p)$$

where g is the gravity force.

Once all the system's energies are obtained, Lagrange's equations can be written as in (3) and (4). The generalized coordinates chosen are the angles $q_1 = \theta_s$ and $q_2 = \theta_p$. Considering that a DC motor attached to the main shaft is used to move the pendulum to drive the spherical robot, it can be assumed τ as the torque generated by the DC motor

Parameter	Symbol	Value
Mass of the sphere	M_s	$0.5kg$
Mass of the pendulum	M_p	$0.639kg$
Radius of the sphere	r	$0.2m$
Distance between the CM of the sphere and the CM of pendulum	l	$0.18m$
Angle of the sphere	θ_s	θ_s
Angle of the pendulum	θ_p	θ_p
Moment of inertia of the sphere	J_s	$0.536kg \cdot m^2$
Moment of inertia of the pendulum	J_p	$0.00277kg \cdot m^2$
Angular velocity of the sphere	ω_s	ω_s
Angular velocity of the pendulum	ω_p	ω_p
Friction force	F_f	F_f
Torque of the motor	τ	τ

Table 1: Parameters of the spherical robot

and F_f as the friction force between the spherical robot and the surface on which it moves. The mathematical model is given by (5).

$$\frac{d}{dt} \left(\frac{\partial \mathcal{L}}{\partial \dot{q}_1} \right) - \frac{\partial \mathcal{L}}{\partial q_1} = Q_1 \quad (3)$$

$$\frac{d}{dt} \left(\frac{\partial \mathcal{L}}{\partial \dot{q}_2} \right) - \frac{\partial \mathcal{L}}{\partial q_2} = Q_2 \quad (4)$$

$$\begin{aligned}
F_f - \tau &= (J_s + J_p + M_p l^2 + (M_s + M_p) r^2 \\
&\quad - 2M_p r l \cos(\theta_s + \theta_p)) \dot{\omega}_s \\
&\quad + (J_p + M_p l^2 - M_p r l \cos(\theta_s + \theta_p)) \dot{\omega}_p \\
&\quad + M_p l \sin(\theta_s + \theta_p) (g + r(\omega_s + \omega_p)^2) \\
\tau &= M_s g l \sin(\theta_s + \theta_p) + (J_p + M_s l^2) (\dot{\omega}_s + \dot{\omega}_p) \\
&\quad - M_s r l \dot{\omega}_s \cos(\theta_s + \theta_p)
\end{aligned} \quad (5)$$

3.1 Motion control using stochastic signals

The spherical robot used for this work performs two kinds of motion: longitudinal and lateral. Using DC motors, we control both motions. One is attached to the main shaft that passes through the case for longitudinal motion, and the second is connected to

the pendulum's rod to conduct steering motion. We employ PID controllers to control the two DC motors. However, the tune of the first one is carried out through stochastic signals [Hasdorff 75, Matus-Vargas et al. 20] that allow us to better deal with irregular surfaces, and the second one is tuned classically. In the case of the first motor, the torque is the manipulated variable, and for the second one, we control its position through the angular velocity.

According to [Hasdorff 75], a random number generation followed by a hold connected to a linear filter $w(t)$ whose transfer function is $W(s)$ that allows limiting the bandwidth of the signals not to alter the integration method that calculates the response of the system.

The setpoint ω_{ssp} and the pendulum's velocity angular ω_p are disturbed by noise. To generate the disturbance signal $d_1(t)$ for the setpoint, we use a second-order filter given by

$$W_2(s) = \frac{24.73}{s^2 + 0.1651s + 24.73} \quad (6)$$

By analysing the poles of the system, we obtained the damping factor $\zeta = 0.01651$ and the natural frequency $\omega_n = 4.973$. In the case of ω_p we use the first order filter (7) to generate the disturbance signal $d_2(t)$ with $a_0 = 1$, which means the disturbance spectrum is mainly flat. The cost function is considered as (8).

$$W_1(s) = \frac{1}{s + a_0} \quad (7)$$

$$J(u) = \int_{t_0}^{t_f} [(\omega_{ssp} - \omega_s)^2 + R (k_p^2 + k_I^2 + k_d^2)] dt \quad (8)$$

$R > 0$ is a scalar constant to vary the weighting on control-effort expense during the interval $[t_0, t_f]$.

4 Motion on irregular surfaces

In this work, we focus on the scenario where the PDSR is required to roll over irregular surfaces whose slope can be variable and inclined. We propose some surfaces to test the robot using the Webots©virtual environment. The first surface corresponds to a ramp whose slope is being incremented by one grade each meter, as shown in Figure 3. The second surface is a variation of the one proposed in [Moazami et al. 19a]. We use the function defined by (9), whose surface is shown in Figure 4.

$$f(x, y) = -0.025(\cos(2x) + \cos(2y) - 2) \quad (9)$$

It is necessary to calculate the slope angles on which the spherical robot moves to roll over these surfaces. Due to all components of the spherical robot moving (the case is rolling, and the transversal shaft is oscillating), it is not possible to measure the slope angle using sensors. We have proposed an alternative that uses the GPS embedded in the spherical robot (Figure 5). It considers a horizontal vector $\overrightarrow{P_0P_1}$, where P_0 is the location of the center of mass at instant $t - 1$ and P_1 is a point located just in front of the previous point. Q is the location of the center of mass of the spherical robot at the current time t , so the angle α can be calculated using (10).

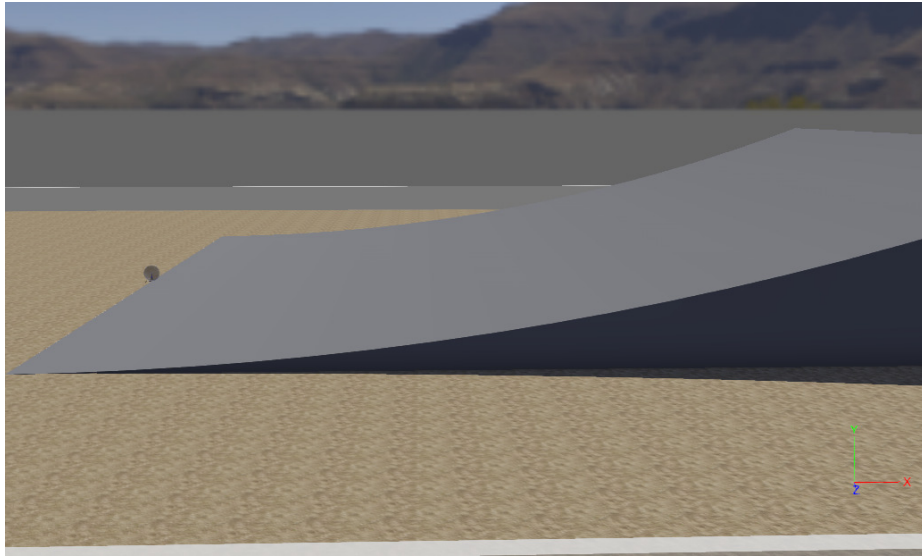


Figure 3: Ramp with increasing slope, side view

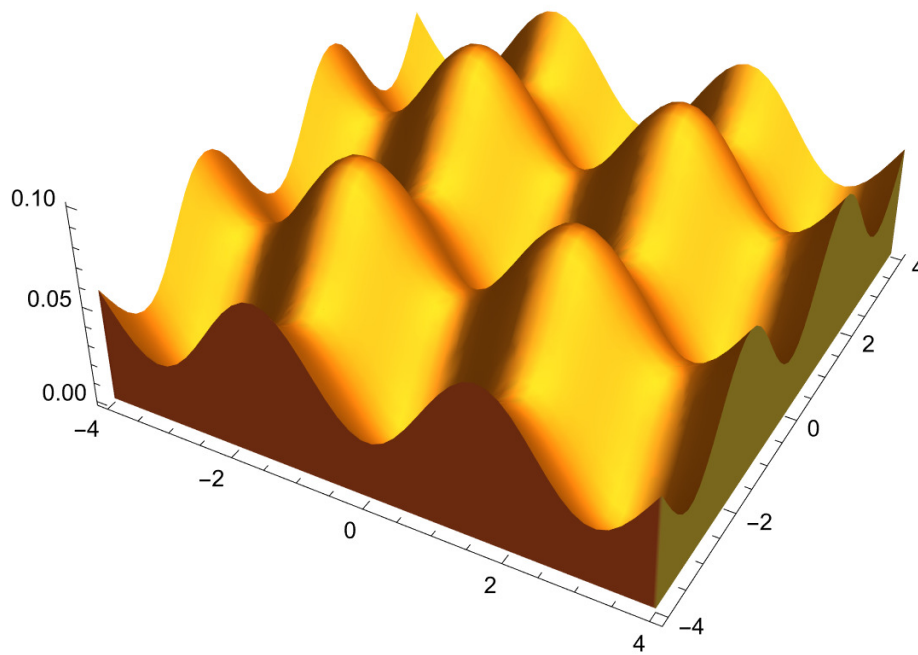


Figure 4: Surface generated using (9), [Moazami et al. 19a]

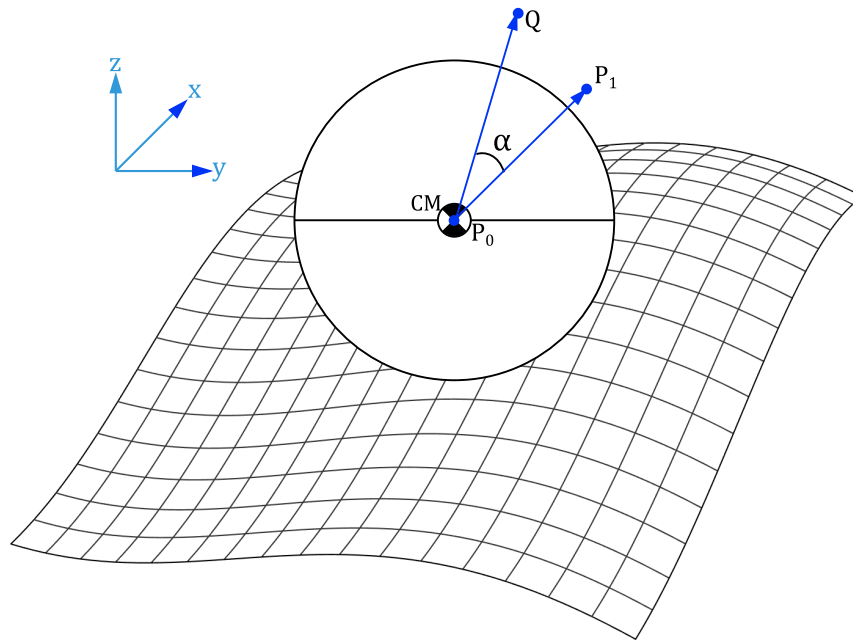


Figure 5: Measuring angles using GPS

$$\alpha = \cos^{-1} \left(\frac{\overrightarrow{P_0P_1} \cdot \overrightarrow{P_0Q}}{|\overrightarrow{P_0P_1}| \cdot |\overrightarrow{P_0Q}|} \right) \quad (10)$$

where $P_0 = (x_{t-1}, y_{t-1}, z_{t-1})$, $P_1 = (x_t, y_t, z_{t-1})$, and $Q = (x_t, y_t, z_t)$.

If the spherical robot is on horizontal surfaces, the motor DC torque is limited to $0.1N \cdot m$ to perform the longitudinal motion. However, on surfaces where the slope increases, the torque value should be increased to reach the angular velocity to enable it to roll over on this type of surface. Table 2 shows some values used to test the torque for different angles of inclination. We interpolated these values using linear least squares regression as shown in Figure 6 to get a factor c that allows us to predict the value of the torque to be applied to the DC motor considering the measured angle.

5 Trajectory tracking

The spherical robot cannot reach targets ahead of it that are not located on its longitudinal axis of travel due to non-holonomic constraints. Suppose the target is contained in the left or right half-plane concerning the longitudinal axis. In that case, we must advance it to the point of intersection of the axis that passes through the target and is orthogonal to the longitudinal axis of the robot. Then, we need to perform steering motion following a semicircle with a given curvature radius ρ , as shown in Figure 7. Through a shift of the center of mass caused by the lateral inclination of the pendulum, it is possible to enable the spherical robot to reach the goal point.

Angles (°)	Maximum Torque (N · m)
2	0.1
4	0.2
6	0.3
8	0.4
10	0.5
12	0.6
14	0.7
16	0.8

Table 2: Angle of inclination of the plane and torque applied

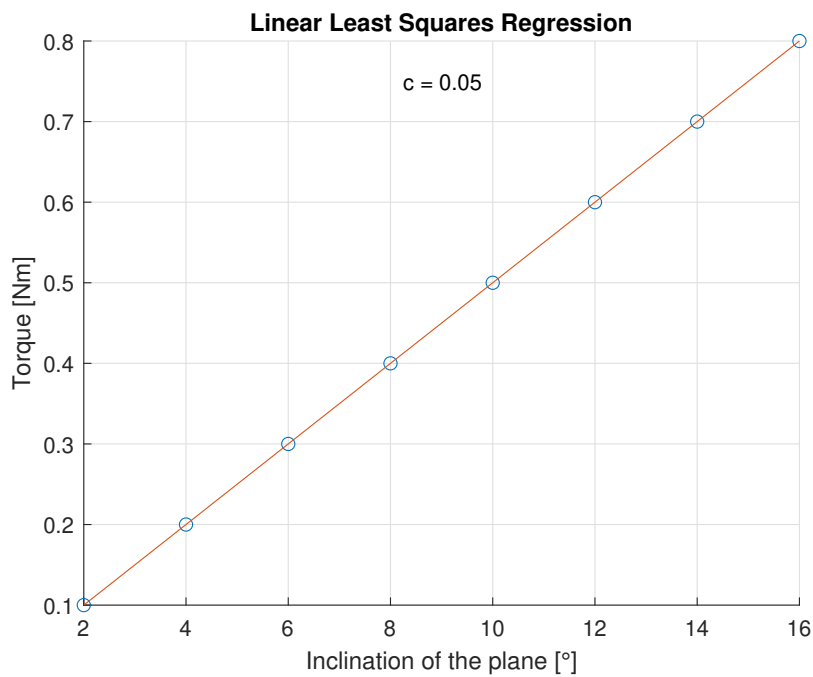


Figure 6: Linear least squares regression

Across the GPS, we get the coordinates of the robot's contact point with the surface and of the target point $\mathbf{x} = (x_1, y_1)$ respectively. Here, we find the curvature radius using the Euclidean distance between both points; see (12) and (13).

$$\gamma = \frac{r\dot{\theta}_r^2(J_s - M_p r l + r^2(M_s + M_p))}{M_p g l \rho} \tag{11}$$

$$\|\mathbf{x} - \mathbf{y}\| = \sqrt{(x_2 - x_1)^2 + (y_2 - y_1)^2} \tag{12}$$

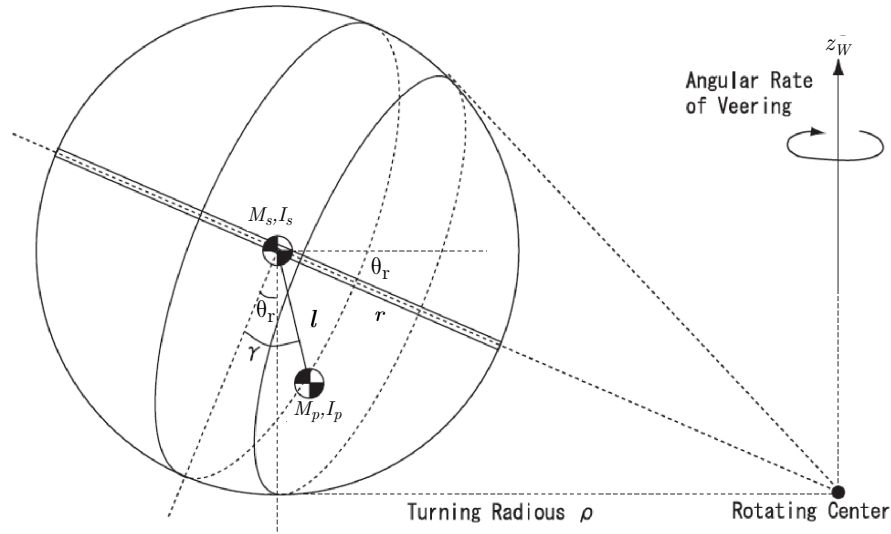


Figure 7: Steering motion of the spherical robot

$$\rho = \frac{\|\mathbf{x} - \mathbf{y}\|}{2} \quad (13)$$

We use the complementary filter (14) to reduce the sideways oscillations caused by the tilting of the pendulum of the robot when it is performing steering motion [Landa and Pilat 16]. The angle $\gamma_{(n)}$ in (14) is got by (11), $\theta_{rm(n)}$ is the angle of inclination of the pendulum, and $\omega_{rm(n)}$ is its angular velocity. We get $\omega_{rm(n)}$ through a position sensor and a gyro located on the second motor. The design parameter ϵ of (14), it is tuned as 0.01, t_s is the sample time of the simulator, and it is equal to 0.032.

$$\gamma_{(n+1)} = (1 - \epsilon)(\gamma_{(n)} + t_s \omega_{rm(n)}) + \epsilon \theta_{rm(n)} \quad (14)$$

6 Simulation Results

This section presents the simulation results of the designed trajectories for the PDSR to meet different targets and change its orientation. In addition, we present the implementation of the PID controls for both DC motors.

6.1 PID motion control

We use a PID controller to control the longitudinal motion through the angular velocity of the robot ω_s . The manipulated variable is the torque τ , and the controlled variable is ω_s . The control is tuning using stochastic test signals that overcome the constraints imposed by step inputs. The transfer function from the motor DC torque τ to the angular

velocity ω_s is obtained from the linearization of (5) [Sanchez-Solar et al. 21]

$$\frac{\Omega_s}{T} = \frac{-(18.17s^2 + 522.86)}{s^3 + 1.64s^2 + 24.98s + 36.6} \quad (15)$$

where Ω_s and T are the Laplace transform of ω_s y τ . The state-space model of the robot spherical obtain from (15) is as follows:

$$\dot{x} = \begin{bmatrix} 0 & 1 & 0 \\ 0 & 0 & 1 \\ -36.6 & -24.98 & -1.64 \end{bmatrix} \begin{bmatrix} x_1 \\ x_2 \\ x_3 \end{bmatrix} + \begin{bmatrix} 0 \\ 0 \\ 1 \end{bmatrix} u \quad (16)$$

$$y(t) = [-522.86 \quad 0 \quad -18.16](x_1, x_2, x_3)^T$$

To find the control gains k_p, k_I, k_d , we use the simulation-based optimization methodology. Given an input control, first, we simulate the physical process given by (16) over $[0, 15]$; second, we evaluate the cost function (8) in the state final reached; third, we use the Polak-Ribiere conjugate gradient method to find the control gains [Hasdorff 75, Matus-Vargas et al. 20].

The initial guess used to the conjugate gradient method is $k_p = -18, k_I = -1, k_d = 1$, the parameter $R = 1 \times 10^{-9}$ (see (8)). To approximate the numerical solution, we use a step fixed fourth order Runge–Kutta method with integration step $\Delta t = 0.01$. The initial condition of the linear model (16) are $(0, 0, 0)$. The disturbance signals $d_1(t)$ and $d_2(t)$ have a mean and variance of $\mu = 0$ and $\sigma^2 = 10, \mu = 0$, and $\sigma^2 = 3$ respectively. The root-mean-square error (RMSE) of $e = \omega_{ssp} + d_1(t) - \omega_s$, and the control gains k_p, k_I, k_d are depicted in Table 3.

k_p	k_I	k_d	RMSE
-43.77	-2.90	-0.22	0.15

Table 3: Controller gains for the first motor

Figure 9 displays the performance of the optimized PID controller with stochastic test signals. The angular velocity ω_s is very similar to the disturbing set point $\omega_{ssp} + d_1(t)$, the behavior is following its RMS of 0.15. Stochastic PID controller outperforms Ziegler-Nichols PID since the Ziegler controller response has an overshoot of 16%, and a settling time of 0.4s. Stochastic PID controller does not have overshoot, and his settling time is almost 0. The comparison between both PID controllers is presented in Figure 8.

The second PID was tuned manually, this is, by trial and error, and had different values for each irregular surface and for each section or semicircle of the trajectory. The values for both surfaces are presented in Table 4.

6.2 Virtual environment

We simulate the spherical robot moving over two irregular surfaces in the virtual environment Webots© to verify if the robot can follow the design trajectories to meet its targets. The first surface is generated by (9), and the second by (17). Figures 10a and 10b depict both surfaces, and the second surface has steeper slopes than the first.

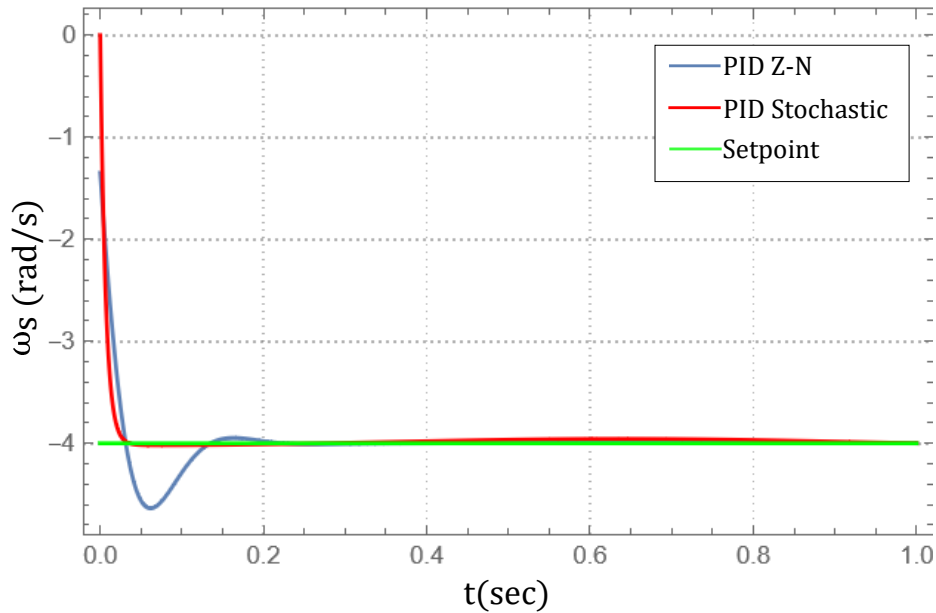


Figure 8: Comparison between PID Z-N and PID Stochastic

Trajectory	Section	k_p	k_I	k_d
1	1	0.048	0.0003	0.003
	2	0.01	0.00131	0.0001
	3	0.3	0.2	0.1
2	1	0.01	0.00005	0.17
	2	1	0	0
	3	0.5	0.01	0.01

Table 4: Controller gains for second motor

$$f(x, y) = -0.1(\cos(2x) + \cos(2y) - 2) \quad (17)$$

Figure 11 depicts the desired trajectory to be followed by the spherical robot over the irregular surface. It consists of three semicircular trajectories to change the orientation of the spherical robot. Due to its non-holonomic constraints, it is not capable of turning around its z axis. The angular velocity of the robot is -4rad/s .

From simulations that can be consulted on a video file located at [this link](#), and from Figure 12 we can observe that for the first surface, the robot reaches the desired goals and ends up facing the opposite direction to the initial. The PID gains for both DC motors are adequate to stabilize the motion of the spherical robot and to face the slopes whose angle is constantly changing in magnitude and direction (from positive to negative and vice versa).

For the second surface, as is shown in Figure 13 we can observe that it is more

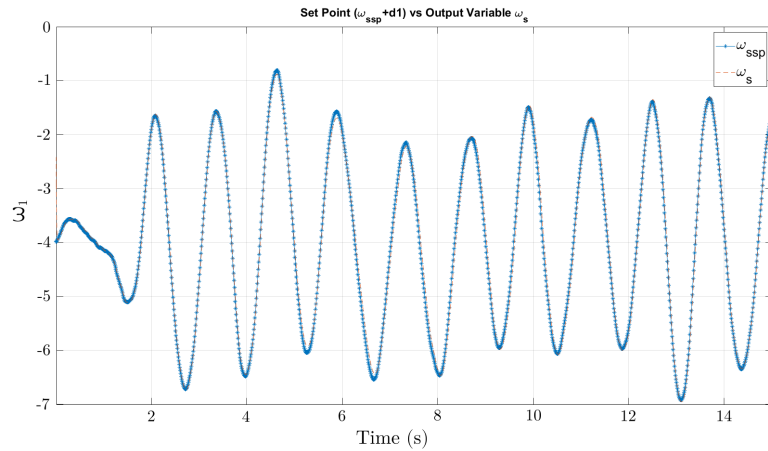
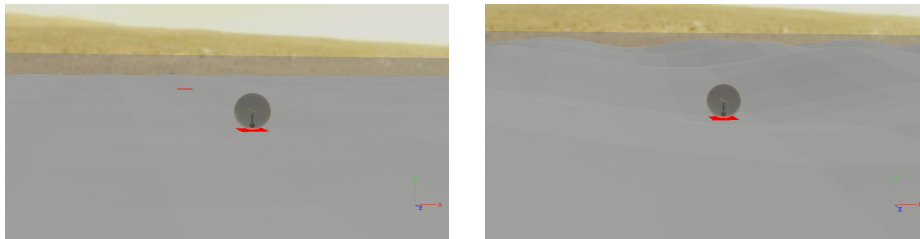


Figure 9: The Performance of the PID Controller ω_s, ω_{ssp}



(a) First surface for tests (low slopes)

(b) Second surface for tests (high slopes)

Figure 10: Proposed surfaces for following trajectories

difficult for the robot to follow the given trajectory because the slopes are more inclined than on the first surface. Even for the second semicircle, the robot exhibits some unstable motion, but the controller manages to stabilize it again. Despite the fact that the trajectory executed is a little further away from the proposed semicircles, the robot reaches all the desired points and changes its initial direction using the proposed trajectory, overcoming the restriction of yaw motion.

7 Conclusions and future work

We have presented an approach to enable a Pendulum-Driven Spherical Robot to overcome the non-holonomic constraints that do not allow it to perform a backward motion. We propose to use alternative trajectories to change its orientation. That is a point of view that had not been considered by other authors such as [Nagai 08], [Roozegar and Mahjoob 17], [Ivanova et al. 18a]. The scenario of reaching goals located on the environment through trajectory planning considering a 2D motion on inclined irregular surfaces changing over time had also not been considered. These are relevant scenarios when the spherical robot is deployed over realistic environments.

Therefore, our approach enables the PDSR to describe semicircles taking advantage of the steering motion that can be produced on the robot by tilting its central pendulum

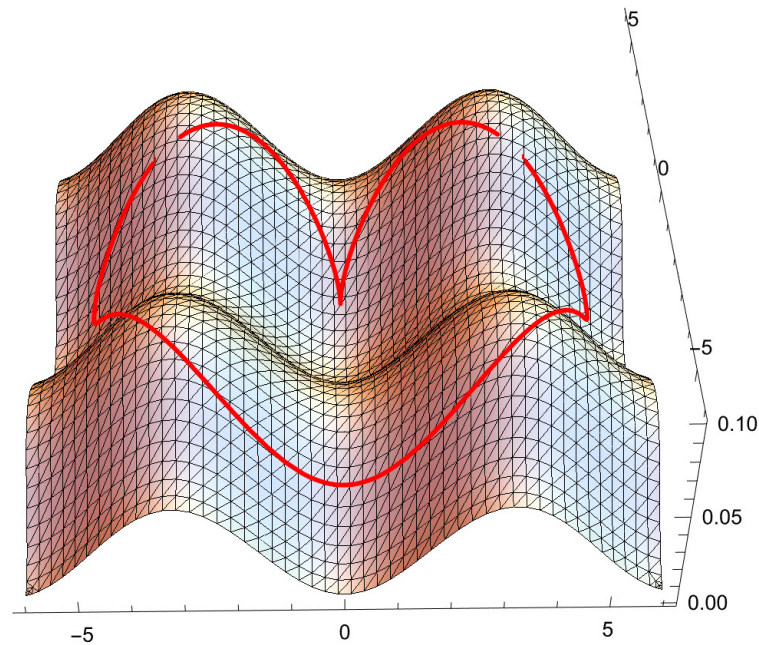


Figure 11: Trajectory proposed to be followed by the spherical robot on an irregular surface

to change its center of mass. Even though it takes a long time to reach all the points to produce backward motion in comparison to other configurations of the spherical robot, such as more pendulums, gyroscopes attached to the pendulum, or hybrid driving mechanisms, the proposed method using semicircular trajectories gives an alternative to overcome the non-holonomic constraints of the system. Besides, it maintains the advantages of using a simple pendulum (less energy consumption, fewer restrictions on manufacturing materials, and fewer actuators to control). Let us compare the time to complete the trajectory to perform backward motion among the spherical robot rolling on a horizontal surface, a smooth irregular surface, and a steep irregular surface. It is possible to obtain a constant representing the ratio between the times obtained in the models. For example, the trajectory on a horizontal surface (T_H) takes about 50s, on a smooth irregular surface (T_{SI}) 67s and on a steep irregular surface (T_{StI}) 86s. It means that $T_{SI} = 1.34T_H$. In other words, the trajectory on a smooth irregular surface is 1.34 times slower than the trajectory on a horizontal surface. In the second case (trajectory on a horizontal surface vs. trajectory on a steep irregular surface), the ratio is given by

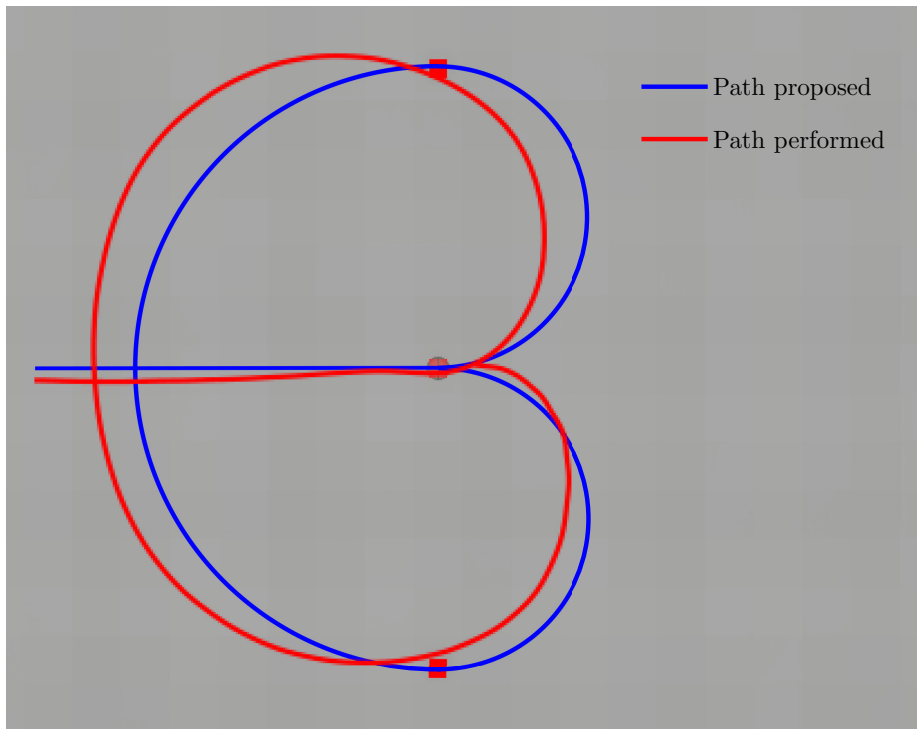


Figure 12: Comparison between the proposed and performed path for the first surface

$T_{StI} = 1.72T_H$, which means that the trajectory on a steep irregular surface is about 1.72 times slower than on a horizontal plane. A drawback in our strategy is noted under the scenario of tuning the parameters of the PID control for the second DC motor, which has to be made for each desired trajectory. Nevertheless, the first DC motor (tuned by using stochastic signals to deal with destabilization caused by varying its torque) is able to maintain the angular velocity of the robot close to the desired value of $-4rad/s$.

One of the most relevant contributions of this research work is that only PID controllers are being used in comparison with other works that use more complex methods to control the spherical robot. The main advantage of using PID controllers are that only the controlled variable needs to be sensed. This results in the use of a smaller amount of components to be included inside the spherical shell. If it is considered that the main environment in which it is intended to perform navigation and exploration is the outer space, then it results in less energy consumption and fewer sensors to be installed in the spherical robot.

It is important to consider that for the first motor, the parameter to be controlled is the angular velocity, which is done by manipulating the torque applied to the motor. For the second motor, the angular velocity is manipulated to obtain the desired value on the second motor's position to reach the pendulum's desired inclination.

For our future work, we propose to apply the same approach of controlling the torque of the second motor by using stochastic signals. To deal with the problem of manual re-tuning of the second PID controller, we will explore the use of AI algorithms such as

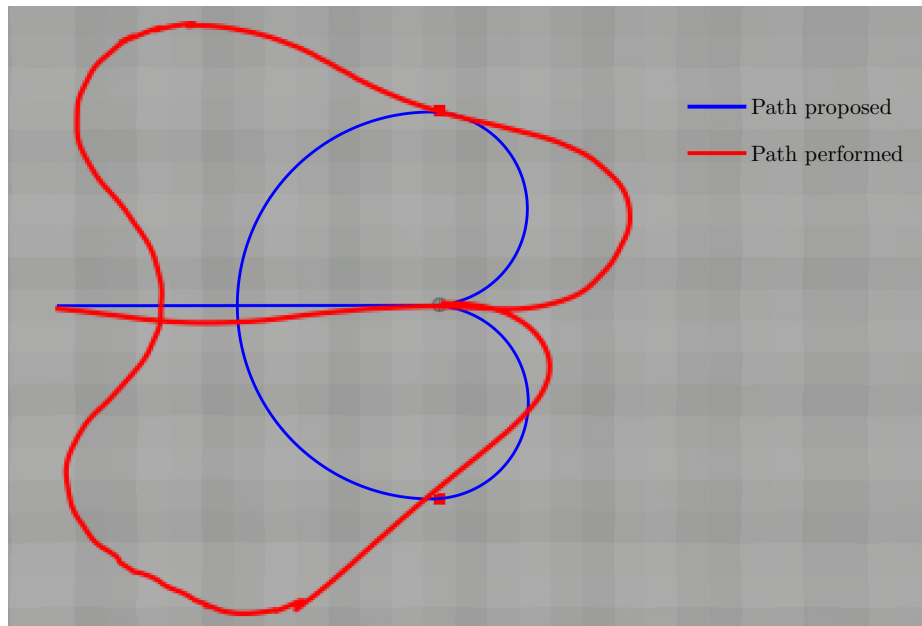


Figure 13: Comparison between the proposed and performed path for the second surface

Deep Learning or Reinforcement Learning.

Acknowledgements

The first author thanks the Consejo Nacional de Ciencia y Tecnología (CONACYT) for the support provided through scholarship number 486961.

References

- [Aalipour et al. 20] Aalipour, M., Mokhtarian, A., Karimpour, H.: Nonlinear control of motion of a spherical robot on inclined surfaces based on feedback linearization method. *Journal Of Applied and Computational Sciences in Mechanics*, 31(2):91–104 (2020).
- [Chase and Pandya 12] Chase, R., Pandya, A.: A review of active mechanical driving principles of spherical robots. *Robotics*, 1(1):3–23 (2012).
- [Halme et al. 96] Halme, A., Suomela, J., Schönberg, T., Wang, Y.: A spherical mobile micro-robot for scientific applications. In *4th ESA Workshop on Advanced Space Technologies for Robot Applications*, Noordwijk, 1996, page 3. The European Space Agency (1996).
- [Hasdorff 75] Hasdorff, L.: *Gradient Optimization and Nonlinear Control*. J.Wiley and Sons, Texas (1975).
- [Ivanova et al. 18a] Ivanova, T. B., Kilin, A. A., Pivovarova, E. N.: Control of the Rolling Motion of a Spherical Robot on an Inclined Plane. *Physics - Doklady*, 63(10):435–440 (2018).

- [Ivanova et al. 18b] Ivanova, T. B., Kilin, A. A., Pivovarova, E. N.: Controlled Motion of a Spherical Robot of Pendulum Type on an Inclined Plane. *Physics - Doklady*, 63(7):302–306 (2018).
- [Koshiyama and Yamafuji 93] Koshiyama, A., Yamafuji, K.: Design and control of an all-direction steering type mobile robot. *The International Journal of Robotics Research*, 12(5):411–419 (1993).
- [Landa and Pilat 16] Landa, K., Pilat, A. K.: Design of a controller for stabilization of spherical robot's sideway oscillations. In 2016 21st International Conference on Methods and Models in Automation and Robotics (MMAR), pages 484–489 (2016).
- [Laplante et al. 07] Laplante, J.-F., Masson, P., Michaud, F.: Analytical longitudinal and lateral models of a spherical rolling robot. Technical report, pages 15–22 (2007).
- [Madhushani et al. 17] Madhushani, T. W. U., Maithripala, D. H. S., Berg, J. M.: Feedback regularization and geometric pid control for trajectory tracking of mechanical systems: Hoop robots on an inclined plane. In 2017 American Control Conference (ACC), pages 3938–3943 (2017).
- [Matus-Vargas et al. 20] Matus-Vargas, A., Rodriguez-Gomez, G., Martinez-Carranza, J.: Parametric Optimization for Nonlinear Quadcopter Control Using Stochastic Test Signals, pages 55–79. Springer International Publishing, Cham (2020).
- [Moazami et al. 19a] Moazami, S., Palanki, S., Zargarzadeh, H.: Kinematics of norma, a spherical robot, rolling over 3d terrains. In 2019 American Control Conference (ACC), pages 1330–1335 (2019).
- [Moazami et al. 19b] Moazami, S., Zargarzadeh, H., Palanki, S.: Kinematics of Spherical Robots Rolling over 3D Terrains. *Complexity*, 2019:1–14 (2019).
- [Nagai 08] Nagai, M.: Control system for a spherical robot. Master's thesis, Helsinki University of Technology (2008).
- [Ocampo 10] Ocampo, J.: Modelo de robot esférico para la locomoción en superficies irregulares. Master's thesis, Instituto Nacional de Astrofísica, Óptica y Electrónica (INAOE) (2010).
- [Ocampo-Jiménez et al. 14] Ocampo-Jiménez, J., Muñoz-Meléndez, A., Rodríguez-Gómez, G.: Extending a spherical robot for dealing with irregular surfaces: a sea urchin-like robot. *Advanced Robotics*, 28(22):1475–1485 (2014).
- [Roозegar et al. 17] Roозegar, M., Ayati, M., Mahjoob, M.: Mathematical modelling and control of a nonholonomic spherical robot on a variable-slope inclined plane using terminal sliding mode control. *Nonlinear Dynamics*, 90(2):971–981 (2017).
- [Roозegar and Mahjoob 17] Roозegar, M., Mahjoob, M. J.: Modelling and control of a non-holonomic pendulum-driven spherical robot moving on an inclined plane: simulation and experimental results. *IET Control Theory & Applications*, 11(4):541–549 (2017).
- [Sanchez-Solar et al. 21] Sanchez-Solar, S.-D., Rodriguez-Gomez, G., Muñoz-Melendez, A., Martinez-Carranza, J.: Tuning, control and path planning of a spherical robot using stochastic signals. In 2021 18th International Conference on Electrical Engineering, Computing Science and Automatic Control (CCE), pages 1–6 (2021).
- [Singhal et al. 23] Singhal, A., Modi, S., Gupta, A., Vachhani, L., Ghag, O. A.: Pendulum actuated spherical robot: Dynamic modeling & analysis for wobble & precession.
- [Tian et al. 23] Tian, X., Xiang, H., Yang, Y., Yan, M., Zhan, Q.: Dynamic model based adaptive sliding mode trajectory tracking control of pendulum-driven spherical mobile robot (2023).
- [Wang et al. 21] Wang, Y., Guan, X., Hu, T., Zhang, Z., Wang, Y., Wang, Z., Liu, Y., Li, G.: Fuzzy pid controller based on yaw angle prediction of a spherical robot. In 2021 IEEE/RSJ International Conference on Intelligent Robots and Systems (IROS), pages 3242–3247 (2021).

[Yu et al. 13] Yu, T., Sun, H., Jia, Q., Zhao, W.: Path following control of a spherical robot rolling on an inclined plane. *Sensors & Transducers*, 21(5):42 (2013).

[Yu et al. 11] Yu, T., Sun, H., Zhang, Y.: Dynamic analysis of a spherical mobile robot in rough terrains. In Pham, K. D., Zmuda, H., Cox, J. L., Meyer, G. J., editors, *Sensors and Systems for Space Applications IV*, volume 8044, pages 269 – 277. International Society for Optics and Photonics, SPIE (2011).

[Zhang et al. 21] Zhang, Z., Wan, Y., Wang, Y., Guan, X., Ren, W., Li, G.: Improved hybrid a* path planning method for spherical mobile robot based on pendulum. *International Journal of Advanced Robotic Systems*, 18(1):1729881421992958 (2021).